NUCLEAR
INSTRUMENTS
& METHODS
IN PHYSICS
RESEARCH
Section A

ELSEVIER

Cherenkov imaging and timing techniques in astroparticle physics

Ch. Spiering

DESY Institute for High Energy Physics, 15538 Zeuthen, Germany

Abstract

Cherenkov techniques are widely used in astroparticle physics experiments. Classical ring imaging has been applied in balloon experiments. Underground Cherenkov detectors also yield ring-like patterns of photomultiplier hits, whereas in deep underwater experiments tracks are reconstructed from the light arrival times at photomultipliers spread over a large volume. Cherenkov air shower detectors either analyze the image of extended showers, or sample the arrival times of the Cherenkov light cone at different points at the earth's surface. This report reviews the various techniques and illustrates them by selected physics results.

1. Introduction

A variety of sophisticated Cherenkov techniques has been developed in the field of astroparticle physics. Classical ring imaging, RICH, has been applied in balloon-born experiments, which are discussed in Section 2. Quite different to RICH is the technique of ground-based air Cherenkov telescopes (ACT). After an infancy period of nearly three decades, in 1989 the first statistically significant detection of a TeV source of γ-rays by *focal plane imaging* of Cherenkov light from the γ-initiated air shower was reported [1]. Imaging is done by one or several mirrors directed to the source, with a matrix of photomultipliers (PMTs) in the focal plane. The light pattern is analyzed to reconstruct the shower axis and to reject the hadronic cosmic ray background. In contrast to the shower imaging method, timing air Cherenkov telescopes (TACT) use extended arrays of PMTs with light collectors to sample the arrival time and amplitude of the Cherenkov light cone at different points. With presently four unambiguously identified TeV γ sources, these techniques are beginning to reveal their enormous discovery potential. Section 3 describes the air Cherenkov methods and sketches the status of observations.

In deep underground Cherenkov detectors such as KAMIOKANDE [2], PMTs line the inner walls of a water tank. They detect the ring-like pattern of the Cherenkov light emitted by single or showering particles. Pioneering results of this technique are the detection of neutrinos from the supernova SN1987 and of solar neutrinos (Section 4). In contrast to deep underground detectors, deep underwater telescopes use PMTs spread over a large volume. Whereas the much smaller underground detectors are optimized to GeV or sub-GeV energies, deep underwater telescopes are tailored to the

TeV scale. Although the idea of deep underwater detectors was formulated more than three decades ago, the method went through a paradoxically long incubation period until 1993, at which time the first small stationary underwater array started operation in Lake Baikal [3]. Many technical and methodical details still have to be investigated in order to build a large detector of km² size [4]. In a certain sense, deep underwater neutrino telescopes are entering a period of infancy similar to that of Cherenkov air detectors in the eighties. Section 5 describes the present status of the field.

2. Balloon and satellite experiments

The performance of a large RICH experiment flown on a high altitude balloon in 1991 was reported at the previous RICH workshop [5]. The RICH consisted of a gaseous radiator 3 m in length, with a large spherical mirror focusing the Cherenkov light via two inclined plane mirrors to TMAE drift chambers as photon detectors. The capabilities of this experiment were limited due to the absence of an analyzing magnet for tracking. CAPRICE, the Cosmic AntiParticle Imaging Experiment presented at this conference [6], includes a spectrometer with a superconducting magnet of 3 T maximum field, multiwire proportional chambers (MWPC) and drift chambers, a time-of-flight system, an electromagnetic calorimeter, and a RICH [7]. With a 10 mm NaF radiator and a 30 mm expansion zone, the RICH is very compact. The photon detector is a TMAE-filled MWPC with pad readout. The detector flew on a stratospheric balloon 8–9 August 1994. First analysis results impressively demonstrate the capability of the system to separate antiparticles such as antiprotons and positrons from the huge bulk of protons, mesons and electrons. A similar RICH detector is discussed

for the AntiMatter Spectrometer in Space, however with the TMAE photon converter replaced by a photocathode made from a thin layer of CsI [8].

3. Ground-based air Cherenkov detectors

High energy cosmic rays interacting with the upper part of the atmosphere initiate extended air showers (EAS). Three techniques are presently used to analyze EAS: air Cherenkov telescopes (ACT) observing the Cherenkov light emitted by the shower, scintillation or tracking chamber arrays sampling the shower tail at ground, and the Fly's Eye technique detecting the faint scintillation light from EAS with energies higher than 100 PeV. A fourth method will be applied in the near future by the MILAGRO Collaboration, aiming to detect EAS through the Cherenkov radiation generated by the shower tail in a big water pool [9].

Charged primary particles do not point back to their sources since they are deflected in the galactic magnetic fields. In contrast, γ-initiated showers can be traced back to their sources. Since γ's contribute less than 1% of all high energy cosmic rays, γ/hadron separation is an essential issue for identification of γ sources.

A shower starts at 20–30 km above ground by primary interaction. The number of secondary particles increases as the shower develops down to 10 km and then decreases. Hadron showers start at lower altitudes than γ showers and have less particles at the position where the latter have their maximum. On the other hand, γ showers fade away earlier than hadron showers. Furthermore, the lateral spread of particles in a γ shower is smaller than in a hadron shower. All of this information can, in principle, be used for γ/hadron discrimination.

The atmosphere is a very specific Cherenkov radiator. Its refraction index is very low and changes with altitude. At a height of 20 km, the Cherenkov angle is $\Theta_c = 0.34°$, whereas for 8 km height $\Theta_c = 0.78°$. As a consequence, Cherenkov light generated between 10 and 25 km height is focussed to a ring of 100–120 m radius; light generated at lower altitudes has impact points closer to the shower axis. Due to the transverse momenta of secondaries, the typical half aperture of the shower cone is about 30 mrad. The Cherenkov light output of a TeV γ shower is about 100 photons/m^2, which has to be compared to starlight background of 160 photons/m^2/20 ns in a 60 mrad cone (all for the spectral range 320–550 nm). The amount of light reaching the ground is roughly proportional to the total energy of the shower.

3.1. Imaging ACTs

In this approach, the Cherenkov light is focussed onto a matrix of PMTs placed at the focal plane of a big reflector. Fig. 1 sketches the principle and Figs. 2a–2d illustrate the position and shape of the images for different cases. The shape of the image can be approximated by an ellipsoid. Its main
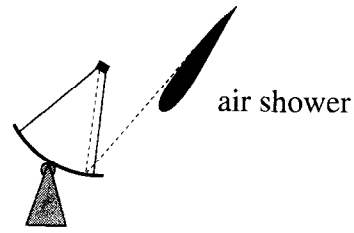

Fig. 1. Principle of imaging ACTs.

direction points to the center of the field of view ($\alpha = 0$) if shower axis and telescope axis are contained in the same plane. Cases (a) and (b) (both with $\alpha = 0$, but shower parallel to telescope axis in case (a), and declined in the common plane towards telescope axis in case (b)) can be distinguished only by stereo imaging, i.e. using a second telescope at some distance to the first. The corresponding ambiguity is partially due to the fact that a radial displacement of the image can also be caused by a varying distance between shower and telescope axis. Knowledge of this distance is important for energy determination and γ/hadron discrimination. A shower with its axis out of a plane containing the telescope plane yields $\alpha \neq 0$ (case (c)). Hadron showers (case (d)) tend to be less collimated than γ showers. The typical angular resolution of ACTs is 0.1–0.2° (about half the pixel size).

The Whipple Observatory (Mount Hopkins, Arizona) has pioneered the imaging technique by operating an array of 37 PMTs in the focal plane of a 10 m diameter optical reflector made from 248 hexagonal mirror facets [1]. The limited resolution of only 37 pixels, each covering 0.5°, did not justify sophisticated image analysis algorithms. Instead, the image was analyzed in terms of some simple parameters [10] explained in Fig. 3. Width and length are proportional to the minor and major axis of the image ellipsoid, respectively. Miss is the distance of the closest approach of the extension of the major axis to the camera center and dist is the distance between ellipsoid center and camera center. Another parameter, azwidth, is the width of the image measured perpendicular to the radius passing through the center of the image. This parameter combines the γ/hadron discrimination power of width (shape) and miss (orientation) and is more effective than either of these criteria act-
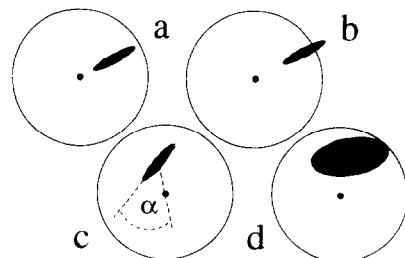

Fig. 2. Images of (a) γ shower, shower axis parallel to telescope axis, (b) γ shower, shower axis in one plane with telescope axis, but declined towards the latter, (c) γ shower, shower axis and telescope axis not contained in same plane, (d) hadron shower.
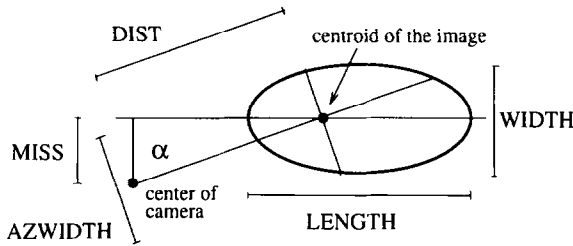
Fig. 3. Definition of image parameters.

ing alone. Whereas hadron showers are expected to peak at *azwidth* $\approx$ 0.3–0.4, ON-source γ showers should give a *azwidth* distribution with a maximum near 0.18–0.2.

In 1989, the Whipple Collaboration reported the first clear observation of a TeV source of γ-rays, the Crab Nebula [1]. Subtracting the normalized *azwidth* distributions of the ON- and OFF-source data, a clear excess at *azwidth* $\approx$ 0.15–0.25 was seen. The significance of the signal was at the 9.0σ level, the corresponding flux $1.8 \times 10^{-11} \gamma \, \text{cm}^{-2} \, \text{s}^{-1}$ above 0.7 TeV. The factor of uncertainty in energy and flux was estimated to be 1.5 at that time. After having upgraded the camera to 91 PMTs (each covering 0.25°), the significance of the signal was steadily improved. Fig. 4 shows the 1992 ON- and OFF-source distributions in the angle α for the Crab Nebula, after application of cuts in the parameters *length*, *width* and *dist* [11]. The excess has a significance of 34σ.

In 1992, the observation of the first extragalactic TeV γ source, the active galaxy Markarian 421, was reported [11]. Mk 421, being a relatively nearby source (redshift=0.031) had been observed before by the EGRET satellite detector at γ energies below 10 GeV. The significance of the Whipple observation ($E > 0.5$ TeV) was 6σ.

Now, the Crab Nebula is accepted as the "standard candle" of ACTs. Four sources of TeV γ-rays have been detected: the
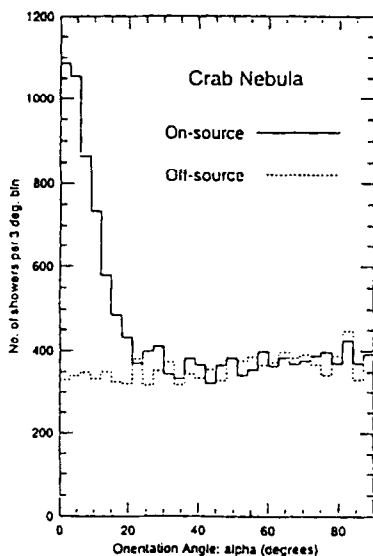

Fig. 4. ON- and OFF-source distributions in orientation angle α for the Crab Nebula, after application of "supercuts" in other image parameters [11].

Crab Nebula, Mk421, the pulsar PSR1706-44 [12] and, very recently, a second extragalactic object, Markarian 501 [23].

The statistical significance of the latter two observations is also convincing – 12σ for PSR1706-44 observed by the 3.8 m CANGAROO telescope in Woomera, Australia, and 10σ for Mk501 observed with the Whipple telescope.

With this clear progress within the last 5–6 years, the imaging ACT technique seems to be a well established method, having indicated its great discovery potential. The main lines of further improvement are:

(i) Smaller and more pixels, yielding a better angular resolution and a better γ/hadron separation both on the trigger and the image analysis level.

Whereas the first Whipple camera consisted of 37 pixels of 0.5°, the CANGAROO camera uses 220 quadratic PMTs, with a pixel size of 0.12°. The camera of the proposed CAT detector in France [14], with 546 pixels each of 0.11°, approaches the ultimate resolution feasible with conventional PMTs. Higher granularity could be reached by multianode photomultipliers. Two telescopes using multianode tubes XP4702 (64 pixels) and XP1704 (96 pixels) have been tested at the EAS-Top site, Gran Sasso [15]. Another possibility is to use image intensifiers with CCD readout [16] (a relatively slow device), or a combination of a fast image intensifier with a matrix of avalanche photodiodes (APDs) [17]. Also, operation of APDs without image intensifiers is discussed [24]. The advantages of this approach are the fine granularity and the high quantum efficiency (up to 80% using APDs with light traps). The main disadvantage is the up-to-now high noise of APDs.

(ii) Larger, or more, mirrors, to collect more light. This would allow the energy threshold to be lowered by about one order of magnitude and to close the energy gap to the EGRET satellite detector which is taking data up to 30 GeV. Expected spectral cutoffs above the energies covered by the EGRET satellite but below the range of present ACTs could indicate the strength of absorption of γ-rays on the intergalactic infrared radiation field.

A very large collector is envisaged within the MAGIC project [24], where one aims to instrument one or more 17 m diameter solar collectors with new mirrors and a high quantum efficiency camera, pushing the threshold down to 10–20 GeV for γ showers! In another approach, multiple distant heliostat mirrors of power plants are used to reflect the Cherenkov light onto a receiver on the central tower of the plant. The receiver consists of secondary optics which focus the light onto a camera of PMTs. This method is pursued by the Solar-One project in California [18], by a project at the THEMIS site in France [25] and by the GRAAL scheme [26] proposing a detector at the CESA-1 heliostat field in Spain.

(iii) Stereo viewing, enabling unambiguous angular measurement, determination of the distance between shower axis and telescope axis, better energy determination and γ/hadron separation.
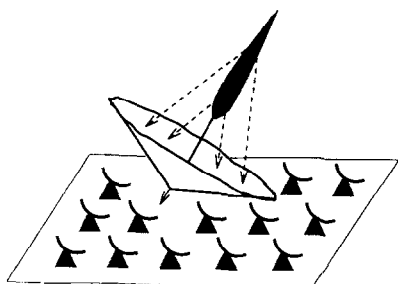
Two-telescope installations are operated, for instance, by

Fig. 5. Schematic view of a TACT with the air shower light cone.

the Whipple group (the 10 m mirror and a new 11 m telescope), the HEGRA group (5 m^2 and 8.5 m^2 at present, plus four additional telescopes in the near future [13]), the CANGAROO-BIGRAT detector [12], and the GT-48 installation in the Crimea [19]. All of these experiments seem to suffer from preliminary difficulties to analyze the data in stereo mode.

(iv) Operation of several telescopes of medium or poor imaging resolution in fast coincidence, allowing lower energy thresholds. This approach is pursued, for instance, by the Durham group [20] using three separate telescopes on a common stand, and by the Noitgedacht detector MK-II in South Africa [22] using telescopes spaced a few hundred meters away.

(v) Reduction of the sensitivity at longer wavelengths to enable observations in moonlight or at twilight. The ultimate approach is to build a telescope sensitive only below 300 nm wavelength.

The Crimean GT-48 detector uses 37-pixel cameras based on solar-blind PMTs [19]. The image intensifier of the Japanese UV Cherenkov Collaboration [16] is equipped with a CsTe photocathode sensitive below 300 nm. The CLUE project under test for several years aims to detect UV photons below 230 nm with the help of proportional chambers filled with TMAE [27].

In an approach presented at this workshop [29], an imaging camera with an upward facing PMT camera is proposed, observing the sky through several apertures in a roof 10 m above the PMTs (*Camera Obscura*). Although, due to its rigidity, it is not suitable for observation of γ point sources, the combination of low noise, wide field of view and good imaging characteristics might help to better determine the energy and the mass composition of very energetic EAS.

3.2. Timing ACTs

To a first approximation, the Cherenkov wave of EAS propagates like a widely open cone with a light front only 3 ns thick. If one arranges many small mirrors over a large area (see Fig. 5), each equipped with a fast PMT, one can fit the time pattern to a conical front model, and determine the main axis of the shower (impact point X, Y and direction angles u, v). The fit also yields the cone opening angle Θ (about 1°) and the arrival time. Furthermore, one can extract the

energy from the amplitude information, in a less ambiguous way than for single-telescope imaging devices. In a certain sense, TACTs are also imaging devices, evaluating, e.g., the radial structure of the wave front in order to discriminate between γ and hadron showers.

The TACT technique has been pioneered by the THEMIS-TOCLE Collaboration, operating 18 parabolic mirror stations at the site of the Themis power plant in the Pyreneés [28]. With an angular resolution of 0.14° and an energy error of only 20% (systematical) and 12–15% (statistical) the group measured the Crab spectrum between 3 and 15 TeV.

All the Cherenkov telescopes mentioned up to now have a rather limited field of view (typically 3–4°). These small-angle telescopes have to be directed to a potential source of γ-rays, and a clear signal is obtained by comparing ON-source and OFF-source measurements. *Wide-angle* ACTs collect the light with PMTs facing towards the sky, with an aperture defined by a collecting reflector like a Winston cone. They can observe a large part of the sky at once, combining ON-source and OFF-source data within the same set of measurements. The first operating wide-angle ACT, dubbed AIROBICC, was built at the HEGRA site at La Palma [30]. The Cherenkov light is sampled by a 7 × 7 matrix of hemispherical 8 in. PMTs with an angular acceptance of 35° (about 1 sr). The angular resolution is 0.2°. Due to the large acceptance, much background light from the night sky is collected. Therefore, the energy threshold has to be kept rather high, about 15 TeV for γ showers. With its rather high threshold, AIROBICC did not observe any γ source up to now. However, with AIROBICC's excellent γ/hadron separation when operated together with the big scintillator array of the HEGRA experiment, a stringent upper limit of 0.8% on the isotropic γ admixture to cosmic rays between 60 and 100 TeV was obtained [31], excluding certain models on cosmic γ production.

A similar, although smaller experiment is operating in the Tunka Valley, Siberia [32]. With this device, as well as with a small-angle TACT in the Tien-Shan [33], the group measured the cosmic particle spectrum up to energies of the order of 10 PeV.

4. Underground Cherenkov detectors

The underground Cherenkov technique has been established by two experiments: the IMB detector, located 1570 meter water equivalent (m.w.e.) underground in a salt mine in Ohio [34] and KAMIOKANDE at a depth of 2700 m.w.e. in the Kamioka mine, Japan [2]. Two huge experiments based on this technique are under construction – the Sudbury Neutrino Observatory in Canada and SUPERKAMIO-KANDE, the 50-kton successor of the present KAMIOKANDE detector. In the following, the principle and successes of the method will be sketched taking the Kamioka detector as an example.
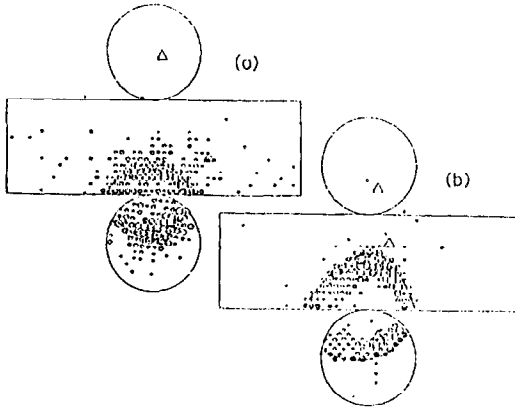
KAMIOKANDE consists of 4.5 kton of purified water in

Fig. 6. Typical Cherenkov patterns of (a) e-like and (b) μ-like events in KAMIOKANDE [36].

a cylindrical tank viewed by roughly 1000 PMTs covering 20% of the surface. With an index of refraction $n = 1.34$, the Cherenkov angle of particles with velocity $\beta \approx 1$ is $\Theta = 42°$. In the wavelength range 300–600 nm, about 3×10^4 photons are emitted per meter track length, yielding typically 10^3 collected photoelectrons. Single Cherenkov rings from *contained events* can be classified as e-like ($e^\pm$, γ) or μ-like ($\mu^\pm$, $\pi^\pm$), by measuring the diffuseness of the rings (see Fig. 6, taken from Ref. [36]). To discriminate low energy μ-like events from e-like events, the information of the opening angle of the Cherenkov ring is used in addition. Time information allows for consistency checks and fine tuning of the results obtained from ring patterns.

Whereas the air Cherenkov telescopes discussed in the previous section are aimed exclusively at EAS detection, underground detectors are multi-purpose devices. According to the typical energy deposition, the following classification can be made for KAMIOKANDE:

7–14 MeV: solar ^{8}B neutrinos, with a huge background of β-rays from the water and γ-rays from the surrounding rock;

5–50 MeV: neutrinos from supernovae, with a background from β and γ emitters and stopping or clipping muons;

$10^2–10^3$ *MeV:* nucleon decays (the original search target of KAMIOKANDE and IMB) and contained atmospheric neutrino events. The background in this region is dominated by stopping muons or muons clipping the detector;

$5 \times 10^2–10^4$ *MeV:* partially contained atmospheric neutrino events, with the main background being due to throughgoing muons;

$5 \times 10^3–5 \times 10^4$ *MeV:* throughgoing muons generated in the atmosphere or by neutrino interactions close to the detector.

Remarkable results have been reported by the KAMIOKANDE Collaboration over the full range of energy sketched above: the ^{8}B flux of neutrinos from the sun has been measured with high accuracy [35]. In 1987, neutrinos from the supernova SN1987 were detected [37]. Stringent lower limits have been set for nucleon life time [38]. The

analysis of contained and partially contained atmospheric neutrino events and the ν_e/ν_μ ratio might indicate neutrino oscillations [36].

5. Deep underwater Cherenkov detectors

No extraterrestrial sources of non-thermal neutrinos have been observed so far. Their existence can be inferred from the observation of charged cosmic particles with energies up to 10^8 TeV. With the exception of the most extreme energies, the origin of these particles can be determined only with the help of neutrinos and γ's, since the directional information of charged particles is washed out by their deflection in the galactic magnetic fields. Underground detectors are too small to detect the feeble fluxes of highly energetic neutrinos from distant "hadron accelerators" such as pulsars or active galactic nuclei (AGN). Underwater detectors can be built much bigger than detectors underground, and with a significantly lower cost-to-area ratio.

Deep underwater Cherenkov telescopes consist of a lattice of PMTs spread over a large volume. Neutrinos are inferred from upward moving muons produced in charged current ν_μ interactions below the detector (I do not regard here shower-like events due to ν_e or neutral current ν_μ interactions). Tracking is done by measuring the arrival times t_i and amplitudes a_i of Cherenkov light at the PMTs and fitting it to the model of a single muon. The fit yields the spatial positions x, y and the crossing time t_0 on a plane where the muon intersects, and the muon direction angles θ and φ. The angular accuracy of the present generation of underwater telescopes will be 1–2°.

Underwater detectors are tailored essentially to the TeV range, for the following reasons: (a) the angle between parent neutrino and muon is $\Theta_\mu \approx 1.5° E_\nu^{-0.5}$ [TeV] enabling source tracing with about 1° accuracy; (b) the neutrino cross section and the muon range increase with energy; (c) above a few TeV, the energy spectrum of neutrinos generated in the atmosphere is considerably steeper ($E^{-3.7}$) than that predicted for extraterrestrial neutrinos (E^{-2}). Therefore, the background from the atmospheric neutrinos with respect to the signal from extraterrestrial neutrinos decreases with energy.

The present generation of underwater neutrino telescopes with planned effective areas of the order of 10^4 m^2 has only limited chances to detect extraterrestrial neutrinos. It is commonly accepted that neutrino astronomy needs a detector of $10^5–10^6$ m^2 size [4]. For the next few years, the only guaranteed source of neutrinos is those generated in the atmosphere. They have to be identified on a vast background of muons also generated in the atmosphere and penetrating down to the detector. The ratio of downward muons to ν-generated upward muons is about 10^6 at a depth of 1 km and 10^4 at a depth of 4 km. The most important aim of the current generation of neutrino detectors is therefore to demonstrate (apart from its technical feasibility, long term reliability, etc.) a sufficient rejection of atmospheric muons

and unambiguous separation of atmospheric neutrino events.

Other physics goals, already attainable in part with the present detector generation, are (a) the search for neutrinos from WIMP annihilation in the sun or the center of the earth; (b) the search for neutrino oscillations using atmospheric or accelerator generated neutrinos; (c) the search for GUT magnetic monopoles catalyzing proton decays; (d) the search for supernova collapses; and (e) cosmic ray physics with downward muons [39].

Four underwater telescopes are presently under construction (for recent reviews see Refs. [40–42]): AMANDA at the South Pole, NT-200 at Lake Baikal, DUMAND near Hawaii and NESTOR near Greece.

BAIKAL. In 1993, the BAIKAL Collaboration installed the first small underwater telescope at a depth of 1.1 km in the Siberian Lake Baikal [3]. NT-36, an array with 36 PMTs, has been in operation for nearly two years, with a slightly changed configuration after recovery, repair and redeployment in 1994. The three strings of NT-36 are attached to a mechanical frame which later will carry the eight strings of a 196-PMT array (NT-200) – see Fig. 7. The optical modules are grouped in pairs along the strings, directed alternatively upward and downward. The two PMTs of a pair are connected in coincidence, giving 18 space points for the NT-36 detector.

The local coincidences are mandatory for the suppression of the background from bioluminescence and PMT noise. The up–down symmetry of the detector allows investigation of the detector performance with downward muons, which are a "calibration source" with known energy and angular spectrum not suffering from statistical limitations. Fig. 8 shows the distribution of the zenith angle θ, for reconstructed muons having passed a fit procedure plus a series of so-
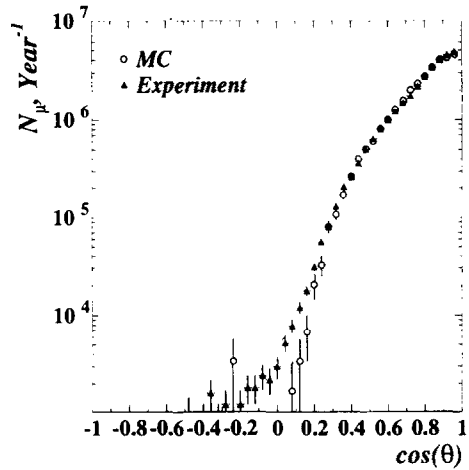
Fig. 8. Zenith angle distribution for reconstructed muons in NT-36. Open circles, MC; triangles, experiment.

phisticated quality criteria [43]. Satisfactory agreement between experimental and Monte Carlo data is observed for $\cos\theta > 0.25$. A small portion of the initial sample is reconstructed as upward moving muons, most of it being fake events (i.e. downward moving muons reconstructed as upward moving). With dedicated up–down cuts, this result is further improved and the ratio of atmospheric neutrino events to fake events is pushed to 1.2×10^{-2}, i.e. there are about 80 fake events per expected neutrino event. Since this is in agreement with MC predictions within a factor of 2, the basic parameters of the array seem to be understood. The limited number of modules, the low dimensionality, and the short lever arm of NT-36 prevent further rejection of the flux of downward moving muons. However, extrapolating the result obtained for NT-36 to a 196-PMT array with eight strings, one obtains a signal-to-noise ratio of better than unity. Thus, NT-36 has provided a certain proof of principle for deep underwater telescopes. Fig. 9 shows one of the tracks reconstructed as an upward muon.

AMANDA. AMANDA [44] is the second project having put into operation a stationary detector. In the austral summer 1993/94, the group froze four strings into the 3 km thick ice at a depth of 0.8–1 km at the South Pole. Among the advantages of the site are the low noise environment of the sterile ice, the unique geographical position and the long absorption length of the ice (seemingly more than 200 m, compared to about 50 m for the deep ocean, and 20 m at Lake Baikal). However, contrary to expectations, at 1 km ice is not yet bubble-free. This results in a light scattering length of 10–20 cm, preventing a proper reconstruction of the Cherenkov cone. In 1995/96, a new telescope will be deployed at greater depth in order to scan the ice properties and hopefully to see the first neutrinos events. The present array is used for supernova search, to study events with high energy deposition and events registered in coincidence with the South Pole surface array SPASE [45].

DUMAND. The goal of the DUMAND-II project is a detector with 216 PMTs at nine strings, at a depth of ≈ 4.5 km
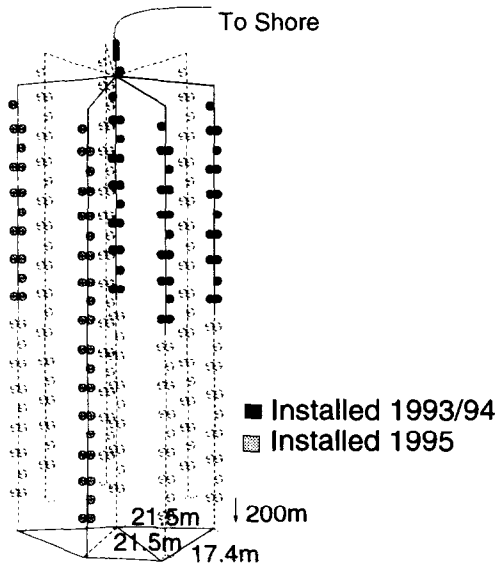

Fig. 7. Schematic view of the planned NT-200 detector. NT-36 components operating since April 1993 are in black, additional modules deployed in March 1995 are in grey.

To Shore

■ Installed 1993/94
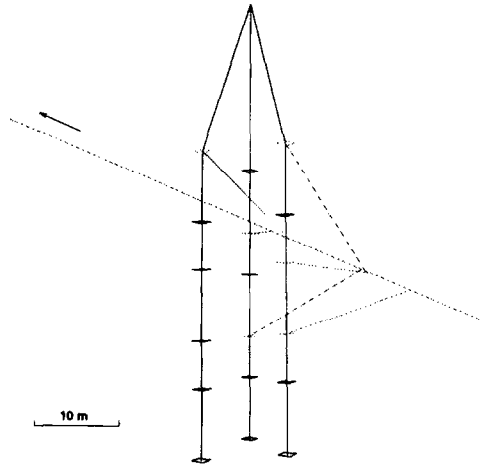▦ Installed 1995

21.5m ↓200m
21.5m 17.4m

Fig. 9. One of the events reconstructed as an upward moving muon track (NT-36, April 1993).

near Hawaii. The project has been active for more than 15 years, defining the physical and methodical problems, carrying out environment studies and creating the necessary technology [46]. In December 1993, the first elements of the telescope were deployed, including a shore cable and one string [47]. Due to a water leak, the string operation ceased after 10 h. The string was released a month later. After careful error analysis, the collaboration envisages the deployment of three strings in 1996.

NESTOR. The detector will be placed at 3.5–4 km depth in the Mediterranean near Pylos, Greece [48]. The 168 PMTs will be fixed on hexagonal floors stacked along a tower-like structure. The up–down symmetry of the array (similar to the Baikal detector) yields a more uniform angular response than those of AMANDA and DUMAND. This is important when searching for neutrino oscillations, either by studying the angular distributions of atmospheric neutrinos or by detecting neutrinos from a beam directed from CERN to the detector site. The NESTOR group has carried out two feasibility tests with single floor arrangements. The first full tower with 12 floors will be deployed in 1997.

Underwater telescopes are "new" detectors, presumably still with a certain period of infancy ahead before evolving to a proven technique. Detectors presently under construction are *prototypes* with respect to one or two detectors of km^2 size to be built in a worldwide effort. The latter goal will be tackled after having demonstrated the neutrino detection capability of the present detectors, and after having understood the basic problems of reliability, scalability of the architecture, parameters of the surrounding medium and real cost.

Acknowledgement

References

[1] T.C. Weekes et al., Astrophys. J. 342 (1989) 379.
[2] K.S. Hirata, Phys. Rev. D 44 (1991) 2241.
[3] I.A. Belolaptikov et al., Nucl. Phys. B (Proc. Suppl.) 35 (1994) 290.
[4] F. Halzen, Nucl. Phys. B (Proc. Suppl.) 38 (1995) 472.
[5] S. Swordy, Nucl. Instr. and Meth. A 343 (1994) 52.
[6] T. Francke, these Proceedings (1995 Int. Workshop on Ring Imaging Cherenkov Detectors, Uppsala, Sweden) Nucl. Instr. and Meth. A 371 (1996) 169.
[7] P. Carlson et al., Nucl. Instr. and Meth. A 349 (1994) 577.
[8] T. Francke, private communication.
[9] D.A. Williams, Proc. 26nd Int. Conf. on High Energy Physics, Dallas, 1992, p. 1197.
[10] A.M. Hillas, Proc. 19th Int. Cosmic Ray Conf., La Iolla, 1985, p. 445.
[11] M. Punch et al., Nature 358 (1992) 477.
[12] T. Tanimori, Proc. Workshop Towards a Major Cherenkov Detector III, ed. T. Kifune, Tokyo, 1994, p. 83.
[13] F. Krennrich, ibid, p. 71.
[14] B. Degrange, ibid, p. 305.
[15] M. Aglietta et al., ibid, p. 101.
[16] R. Susukita, ibid, p. 113.
[17] E. Lorenz, ibid, p. 341.
[18] R.A. Ong et al., ibid, p. 295.
[19] O. Kalekin, A. Stepanian and Yu. Neshpor, ibid, p. 107.
[20] R. Brazier et al., Proc. 21st Int. Cosmic Ray Conf., Adelaide, 1990, p. 274.
[21] P. Goret et al., Proc. 22nd Int. Cosmic Ray Conf., Dublin, 1991, p. 91.
[22] G. Brink et al., ibid, p. 622.
[23] Int. Astron. Union, Circular 6179, 16 June 1995.
[24] S. Bradbury et al., Proc. 24th Int. Cosmic Ray Conf., Rome, 1995, in press.
[25] E. Paré et al., Proc. Heidelberg Workshop on TeV γ Rays, Heidelberg, Oct. 1994.
[26] R. Plaga et al., Proc. 24th Int. Cosmic Ray Conf., Rome, 1995, in press.
[27] B. Bartoli et al., Nucl. Instr. and Meth. A 302 (1991) 515.
[28] P. Baillon, Proc. 26th Int. Conf. on High Energy Physics, Dallas, 1992, p. 1218.
[29] B.A. Khrenov, Ref. [6], p. 174.
[30] M. Bott-Bodenhausen et al., Nucl. Instr. and Meth. A 315 (1992) 236.
[31] A. Karle et al., Phys. Lett. B 347 (1995) 161.
[32] S.V. Brianski et al., Proc. 24th Int. Cosmic Ray Conf., Rome, 1995, in press.
[33] R. Antonov et al., Astropart. Phys. 3 (1995) 231.
[34] R.M. Bionta et al., Phys. Rev. Lett. 51 (198) 27.
[35] K.S. Hirata, Phys. Rev. D 44 (1991) 2241.
[36] T. Kajita, in: Physics and Astrophysics of Neutrinos, eds. M. Fukugita and A. Suzuki (Springer, Berlin, 1994) p. 559.
[37] K.S. Hirata et al., Phys. Rev. Lett. 58 (1987) 1490.
[38] K.S. Hirata et al., Phys. Lett. B 220 (1989) 308.
[39] T. Gaisser, F. Halzen and T. Stanev, Phys. Rep. 258, 3 (1995) 173.
[40] L. Resvanis, Proc. Heidelberg Workshop on TeV γ Rays, Heidelberg, Oct. 94.
[41] S. Barwick, Nucl. Phys. B (Proc. Suppl.) 43 (1995) 183.
[42] Ch. Spiering, talk given at the Baksan School on Physics and Astrophysics, Baksan Valley, Feb. 1995 (in press).
[43] See I. Sokalski and Ch. Spiering (eds.), The Baikal Neutrino Telescope NT-200, Project Description, Baikal-Note 92-03; Belolaptikov et al., papers in Proc. 24th Int. Cosmic Ray Conf., Rome, 1995 (in press).
[44] D.M. Lowder et al., Proc. 23rd Int. Cosmic Ray Conf., Calgary, 1993, p. 569.
[45] See the papers of R. Wischnewski et al., P. Mock et al., and T. Miller et al., submitted to the 24th Int. Cosmic Ray Conf., Rome, 1995, in press.
[46] A. Roberts, Rev. Mod. Phys. 64 (1992) 259.
[47] P. Grieder, Nucl. Phys. (Proc. Suppl.) 43 (1995) 145.
[48] See, e.g., L.K. Resvanis (ed.), Proc. NESTOR Workshop, Pylos, 1992 (University of Athens, Athens, 1993).